Translational Oncology 13 (2020) 100833

Contents lists available at ScienceDirect

Translational Oncology

journal homepage: www.elsevier.com/locate/tranon

MEK blockade overcomes the limited activity of palbociclib in head and neck cancer

Zhenghuan Fang [a,1], Kyung Hee Jung [a,1], Ji Eun Lee [a], Jinhyun Cho [b], Joo Han Lim [b], Soon-Sun Hong [a,*]

[a] Department of Biomedical Sciences, College of Medicine, Inha University, Sinheung-dong, Jung-gu, Incheon 22332, Republic of Korea
[b] Department of Internal Medicine, Inha University Hospital, College of Medicine, Inha University, Sinheung-dong, Jung-gu, Incheon 22332, Republic of Korea

ARTICLE INFO

Article history:
Received 17 May 2020
Received in revised form 25 June 2020
Accepted 30 June 2020
Available online xxxx

ABSTRACT

Head and neck cancer (HNC) is characterized with multiple aberrations in cell cycle pathways, including amplification of cyclin D1. Palbociclib (PAL), a cyclin-dependent kinase 4/6 (CDK4/6) inhibitor, has been reported to regulate cell cycle progression in HNC. However, recent studies have revealed the acquired resistance of certain cells to PAL through activation of the mitogen-activated protein kinase kinase (MEK)/extracellular signal-regulated kinase (ERK) pathway. Therefore, we investigated whether the inhibition of MEK/ERK pathway by trametinib (TRA) may overcome the limited efficacy of PAL in HNC. We evaluated the effect of PAL alone and in combination with TRA on the viability of HNC cells, and found that the combination treatment synergistically inhibited the proliferation of HNC cells. The combination treatment induced G0/G1 cell cycle arrest and apoptotic cell death. In particular, apoptosis mediated by the combination treatment was accompanied with an increase in caspase-3 activity and the number of TUNEL-positive apoptotic cells. These results were consistent with the decrease in cell cycle progression and mitogen-activated protein kinase (MAPK) pathway activation. In a xenograft mouse model of HNC, PAL and TRA synergistically inhibited tumor growth and enhanced tumor cell apoptosis, consistent with the increase in the number of TUNEL-positive cells. The anti-proliferative effects were evident in tumor tissues subjected to the combination treatment as compared with those treated with single drug. Taken together, our study demonstrates that the combination of PAL and TRA exerts synergistic anticancer effects and inhibits cell cycle check points and MEK/ERK pathway in HNC, suggestive of their potential application for HNC treatment.

1. Introduction

Head and neck cancer (HNC), a heterogenous group of cancers, is the sixth most common cancer worldwide. The annual incidence of HNC is approximately 600,000 cases, and the 5-year survival outcome is poor (~50%) [1]. At diagnosis, 45% patients have regional lymph node metastasis, and the chances of development of a second primary tumor in patients with HNC are exceptionally high [2]. Unfortunately, these tumors are often diagnosed only once they have locoregionally advanced; the consequences include poor prognosis [3]. Although various prognostic biomarkers have been identified, there is no widely accepted molecular classification.

Most cancers are characterized with dysregulations in various molecular pathways related to cell cycle. In particular, HNC is largely driven by several molecular changes affecting cell cycle, including amplification of cyclin D1 and loss of p16 gene [4]. Cyclin-dependent kinase 4/6 (CDK4/6) rapidly form complexes with cyclin D and drive cell proliferation. A well-known target of cyclin D-CDK4/6 complex is the retinoblastoma protein [2], which binds and inhibits the activation of E2F transcription factors. Rb phosphorylation promotes the expression of E2F target genes, which initiate cancer cell replication and division [5–7]. In the last decade, a new generation of selective CDK4/6 inhibitors has been developed to target CDK/Rb cell cycle pathway in multiple types of cancers, including melanoma and breast and colorectal cancers [8–10]. Of these, palbociclib (PAL) is a specific CDK4/6 inhibitor and the first-in class drug approved for breast cancer treatment [11]. It arrested cell cycle progression and inhibited tumor growth in preclinical models of HNC [12]. However, CDK4/6 inhibitors such as PAL were cytostatic and induced tumor growth stabilization, but not cytotoxicity in preclinical HNC models [12,13]. Therefore, it is imperative to find an agent that may be potent in combination with CDK4/6 inhibitor to provoke tumor regression. Some studies have evaluated the effect of PAL and cetuximab (an epidermal growth factor receptor [EGFR] inhibitor) in HNC and reported that this combination could synergistically reduce HNC cell viability and regress tumor growth in patients with platinum-resistant HNC in a phase I trial [14,15]. Despite the evidence of clinical response, the development of resistance is common and the mechanism underlying drug resistance is poorly understood. Considering the promising potential of CDK4/6 inhibitors in the clinical setting, it is encouraging to develop a novel therapeutic combination that could effectively inhibit tumor growth and study the underlying mechanism to prevent drug resistance.

* Corresponding author.
E-mail address: hongs@inha.ac.kr. (S.-S. Hong).
[1] These authors equally contributed to this work.

http://dx.doi.org/10.1016/j.tranon.2020.100833

Mitogen-activated protein kinase (MAPK) signaling pathway regulates cell proliferation, survival, and apoptosis [16,17], and the upregulation in mitogen-activated protein kinase kinase (MEK)/extracellular signal-regulated kinase (ERK) pathway is known to accelerate cell proliferation and cell cycle progression through cyclin D transcription [18,19]. Acquired CDK4/6 resistance has been shown to be associated with activation of the MAPK signaling pathway and may confer sensitization to MEK inhibitors [20]. The use of MEK inhibitors is a new treatment strategy for advanced cancers resistant to CDK4/6 inhibitors. Therefore, we sought to develop an effective combination strategy to enhance the anticancer activity of PAL and prevent any acquired resistance to PAL through the blockade of MAPK signaling in a preclinical HNC model. In the present study, we hypothesize that the combination of PAL and trametinib (TRA, a MEK inhibitor) serves as a potent treatment strategy in patients with HNC and overcomes the limited activity of PAL through the blockade of cell cycle progression and MEK/ERK pathways.

2. Materials and methods

2.1. Cells and reagents

Human Detroit 562 and SNU-1076 HNC cells were purchased from the American Type Culture Collection (ATCC, Manassas, VO) and Korean Cell Line Bank (KCLB). Cells were cultured in Eagle's minimum essential medium (EMEM) and Roswell Park Memorial Institute (RPMI)-1640 medium supplemented with 10% fetal bovine serum (FBS) and 1% antibiotic-antimycotic. Cultures were maintained at 37 °C in a 5% CO_2/95% air incubator. The 3-(4,5-dimethylthiazol-2-yl)-2,5-diphenyl tetrazolium bromide (MTT) assay kit was purchased from Sigma Aldrich (St. Louis, MO). PAL (PD332991) and TRA (GSK-1120212) were supplied by LC laboratories and dissolved in dimethyl sulfoxide (DMSO) and stored at −20 °C.

2.2. Measurement of cell viability

The cytotoxic effects of PAL and/or TRA on HNC cells were investigated using the MTT assay. Briefly, Detroit 562 and SNU-1076 cells were seeded at a density of 2.5×10^3 cells/well into 96-well plates and incubated for 24 h at 37 °*C. media* were removed, and the cells were treated with PAL (0.1 or 0.5 μM) and TRA (1 or 5 nM) or the corresponding control reagent (DMSO) for additional 72 h. MTT solution (20 μL, 2 mg/mL) was added to each well, and the cells were incubated for 4 h at 37 °C. The resulting formazan crystals were dissolved in DMSO with constant shaking for 30 min, and the optical density (OD) of each reaction well was measured using a microplate reader at 540 nm wavelength. Three replicate wells were used throughout.

2.3. Three-dimensional (3D) spheroid formation

Detroit 562 and SNU-1076 cells were cultured in flasks at 37 °C and 5% CO_2. The attached cells were trypsinized and seeded into a 96-well ultra-low attachment microplate (Corning) at 1500–2000 cells/well in a complement medium supplemented with basic fibroblast growth factor (bFGF), human epidermal growth factor (hEGF), N-2, and B-27. The cells were incubated for 24 h at 37 °C and then treated with PAL (0.1 or 0.5 μM) and TRA (1 or 5 nM) for 14 days. The diameter of the spheroids formed was measured using a computer software.

2.4. BrdU cell proliferation assay

Detroit 562 and SNU-1076 cells were seeded at 3×10^3 and 2×10^3 cells/well in 96-well plates, respectively. Next day, the media were removed, and the cells were treated with PAL (0.1 or 0.5 μM) and TRA (1 or 5 nM) or the corresponding vehicle (DMSO) for additional 96 h. Following incubation, the cells were treated with a 1× BrdU solution for 4 h at 37 °C and a proliferation assay was performed upon BrdU cell proliferation assay kit (Cell Signaling Technology). Each well was incubated with a fixing/denaturing solution for 30 min at room temperature, and then treated with a 1× BrdU detection antibody solution for 1 h. The cells were washed thrice and incubated with a horseradish peroxidase (HRP)-conjugated antibody solution for 30 min, followed by washing using a washing buffer. Tetramethylbenzidine (TMB) substrate was added to each well for 20 min reaction, then it was terminated with the addition of 2 N sulfuric acid. Absorbance was recorded at 450 nm wavelength using a microplate reader.

2.5. Clonogenic assay

Detroit 562 and SNU-1076 cells were seeded at a density of 2×10^5 cells in 6-cm dishes and incubated for 24 h at 37 °*C. media* were removed and the cells were treated with PAL (0.1 μM) and/or TRA (5 nM) for 48 h. Cells were re-plated in triplicates at 500 cells/well into six-well plates and incubated for 14 days. Colonies in each well were washed twice with Dulbecco's phosphate-buffered saline (DPBS), fixed with 4% paraformaldehyde (PFA), stained with crystal violet for approximately 20 min, quantified, and photographed.

2.6. Western blot analysis

Cells were washed twice with DPBS and lysed with radioimmunoprecipitation assay (RIPA) buffer (Biosesang, Korea) containing 150 mM sodium chloride (NaCl), 1% Triton X-100, 1% sodium deoxycholate, 0.1% sodium dodecyl sulfate (SDS), 50 mM Tris-HCl (pH 7.5), 2 mM ethylenediaminetetraacetic acid (EDTA; pH 8.0), and Xpert protease inhibitor and phosphatase inhibitor cocktail (GenDEPOT, Barker, TX). Proteins were separated by 8% or 15% SDS- polyacrylamide gel electrophoresis (PAGE), and the separated proteins were transferred onto polyvinylidene fluoride (PVDF) membranes. Transferred proteins were confirmed using a Ponceau S staining solution (AMRESCO, Solon, OH), and the blots were then sequentially incubated with primary antibodies and HRP-conjugated secondary antibodies. Antibody binding was detected using an X-Ray film and enhanced with chemiluminescence (ECL) reagent (Bio-Rad, Hercules, CA). Primary antibodies against p-Rb, Rb, cyclin B1, E2F1, p-ERK, ERK, X-linked inhibitor of apoptosis (XIAP), survivin, and B cell lymphoma (Bcl)-2 were purchased from Cell Signaling Technologies (CST, Beverly, MA), and β-actin antibody was obtained from Sigma Aldrich (Sigma Aldrich, St. Louis, MO). Secondary antibodies were purchased from Cell Signaling Technologies.

2.7. Cell cycle analysis

Cells were fixed in 70% ethanol, re-suspended in DPBS along with RNase A (10 μg/mL), and stained with propidium iodide (PI, 50 μg/mL) for 30 min at 37 °C. Cell cycle portions were analyzed using a fluorescence-activated cell sorting (FACS) analyzer (FACS verse, BD Biosciences, Franklin Lakes, NJ).

2.8. Terminal deoxynucleotidyl transferase dUTP nick end labeling (TUNEL) assay

Apoptotic cell detection was conducted with the ApopTag® Peroxidase In Situ Apoptosis Detection Kit (Merck Millipore, Burlington, MA). Briefly, cells were seeded onto 18-mm cover glasses and cultured up to ~70% confluency over 24 h in 37 °C. Cells were then treated with PAL (5 μM) and/or TRA (50 nM) for 48 h, fixed in an ice-cold mixture of acetic acid and ethanol solution, washed with DPBS, and stained with the TUNEL assay solution. The slides were mounted and examined for nuclear fragmentation under a light microscope.

2.9. Histological and immunohistochemistry analyses

In brief, tumor contained paraffin sections (8-μm) were deparaffinized with two changes of xylene and graded ethanol for 10 min for each step, and subjected to antigen retrieval in 0.01 mol/L sodium citrate using a

microwave for 5 min. Endogenous peroxidase activity in tissues was blocked with 3% hydrogen peroxide (H_2O_2) at room temperature for 10 min. The sections were further blocked with normal goat or horse serum at room temperature (RT) for 1 h, and then incubated with either hematoxylin and eosin (H&E) or specified primary antibodies for overnight at 4 °C. A secondary biotinylated antibody was applied to the slides for 1 h at RT before detection using a HRP antibody detection system or freshly prepared 3′,3′-diaminobenzidine (DAB) as the chromogen (brown). Sections were counterstained, and nucleus was visualized with hematoxylin solution. At least three random fields in each section were examined at a magnification of 200 × .

2.10. Mouse xenograft model

Animal care and experimental procedures were conducted in accordance with the approval and guidelines of the INHA Institutional Animal Care and Use Committee (INHA 171205–528) at Inha University Medical School. The cells were harvested and mixed with PBS (200 μL/mouse). After 1 week of adaptation period, 5-weeks-old male BALB/c nude mice (Orient Bio, Korea) were inoculated with 5×10^6 cells in the right flank to initiate tumor growth. As the tumor size reached approximately 50–100 mm^3, mice were randomly divided into four groups of six mice as follows: group 1, vehicle (control); group 2, PAL (50 mg/kg) only; group 3, TRA (3 mg/kg) only; group 4, combo (PAL and TRA treatment). The mice in the vehicle group were treated with 200 μL of 0.5% carboxymethyl cellulose (CMC) by oral gavage, and those from the treatment groups were administered with PAL (50 mg/kg) or TRA (3 mg/kg) daily for 25 days (oral gavage). The tumor size was measured with fine calipers thrice a week and the tumor volume was calculated using the formula $0.5 \times (\text{length} \times \text{width}^2)$. At the end of the experiment, mice were sacrificed and the primary tumors were harvested, weighed, photographed, and stored at −80 °C.

2.11. Statistical analysis

Results are expressed as the mean ± standard deviation. Statistical analysis was performed using analysis of variance (ANOVA) and the Student's *t*-test. The following symbols were used to indicate significant differences: n.s., $^*P < .05$, $^{**}P < .01$, $^{***}P < .001$ or $^{+}P < .05$, $^{++}P < .01$, $^{+++}P < .001$.

3. Results

3.1. The combination of PAL and TRA synergistically induced cell death in 2D and 3D cultures of HNC cell lines

We evaluated the anticancer activity of PAL and TRA in HNC cells using a cell viability assay. The cells were treated with different concentrations of PAL (0.1 and 0.5 μM) and TRA (1 or 5 nM) for 48 h. Cotreatment with both agents significantly inhibited the growth of cells as compared with the treatment using single agents (Fig. 1A). To identify the synergistic effects of PAL and TRA, we calculated the combination index (CI) values using CompuSyn v1.0 (Biosoft). As shown in Fig. 1B, PAL and TRA showed significant synergistic effects with CI values <1 in SNU-1076 and Detroit 562 HNC cells. To validate the synergistic effects, we examined the efficacy of the combination treatment in 3D spheroid cultures. Spheroid morphology varied from a compact appearance (SNU-1076) to an irregular surface (Detroit 562). Treatment with PAL or TRA alone inhibited the spheroid formation ability of HNC cells by 30–50%, whereas the combination treatment induced approximately 50–70% inhibition (Fig. 1C). These findings show that the drug combination acted in a synergistic manner and may serve as an attractive strategy for treatment of HNC.

3.2. The combination of PAL and TRA synergistically inhibited the proliferation and cycle progression of HNC cell lines

Proliferative index is used as a prognostic parameter of cancer progression, and highly proliferating cells often correlate with poor outcomes. To evaluate the effect of PAL and/or TRA on the proliferation of HNC cells, BrdU cell proliferation assay was performed. Anti-proliferative effects of PAL and TRA were dose-dependently shown in both HNC cell lines (Fig. 2A). In particular, the combination treatment exerted significant anti-proliferative effects as compared with the treatment with single agents (Fig. 2A). We studied the long-term effects of PAL and TRA using the clonogenic assay, and found that the cotreatment could significantly suppress the colony formation ability of both cell types as compared with single agent treatment (Fig. 2B). We also performed cell cycle analysis after the treatment of cancer cells with PAL and TRA. Aside from delayed cell proliferation, the combination treatment group also showed cell cycle arrest in the G1 phase (Fig. 2C).

3.3. The combination of PAL and TRA synergistically inhibited the MAPK/ERK and cell cycle pathways

PAL exerted anti-proliferative effects through inhibition of the components of cell cycle pathway, including Rb and cyclins. TRA exhibits anticancer effects by blocking MEK pathway. Resistance to PAL has been reported to be mediated through activation of the MAPK pathway. Therefore, we investigated whether the combination of TRA and PAL could synergistically inhibit these two pathways. As shown in Fig. 3, the expression levels of p-Rb, Rb, cyclin B1, and E2F decreased in PAL-treated cells and the level of p-ERK decreased in TRA-treated cells. However, we observed that the combination of both drugs could synergistically inhibit these two pathways. TRA combined with PAL almost completely blocked the undesirable activation of ERK, suggesting that TRA may prevent PAL resistance and maximize its anticancer effect.

3.4. The combination of PAL and TRA increased mitochondrial-mediated apoptosis

As the combination treatment with PAL and TRA caused a significant reduction in cell proliferation, we investigated whether it could induce apoptosis of HNC cells. We found that the number of TUNEL-positive cells and the expression of cleaved caspase-3 were higher in the cells cotreated with both drugs than in those treated with single agents (Fig. 4A and B). To further clarify whether the combined treatment induces apoptosis through the mitochondrion-mediated pathway, we analyzed the expression of mitochondrial-related proteins. Cotreatment with PAL and TRA significantly suppressed the expression of anti-apoptotic factors such as Bcl-2, survivin, and XIAP as compared with treatment with single agents (Fig. 4C).

3.5. The combination of PAL and TRA suppressed tumor growth in an HNC xenograft model

To evaluate the antitumor effects of the combination of PAL and TRA, we used a xenograft model of HNC derived from Detroit 562 cells using BALB/*c nu/nu* mice. All treatments were well tolerated and no significant differences were observed in the body weights of mice from different groups. During the treatment for 4 weeks, exposure to PAL or TRA alone delayed tumor growth, but the combination of PAL and TRA could significantly reduce tumor volume. In comparison with the control group, the combination treatment group showed an 86% decrease in tumor growth (Fig. 5A and B). This observation was consistent with the changes in tumor weight and volume (Fig. 5C and D). The combination of PAL and TRA did not lead to a significant increase in levels of aspartate aminotransferase (AST), alanine aminotransferase (ALT), and blood urea nitrogen (BUN) in mice, thus evident of an acceptable toxicity profile (Fig. 5E). Thus, the combination treatment regimen exhibited an acceptable safety profile even after multiple administrations. In the histopathological analysis, the group cotreated with PAL and TRA showed a decrease in the expression of proliferating cell nuclear antigen (PCNA), a cell proliferation marker, as compared with the control group. The combination treatment also increased the number of apoptotic cells in tumor tissues, identified as DNA fragments in TUNEL staining (Fig. 6). As PAL can potentially impede

A

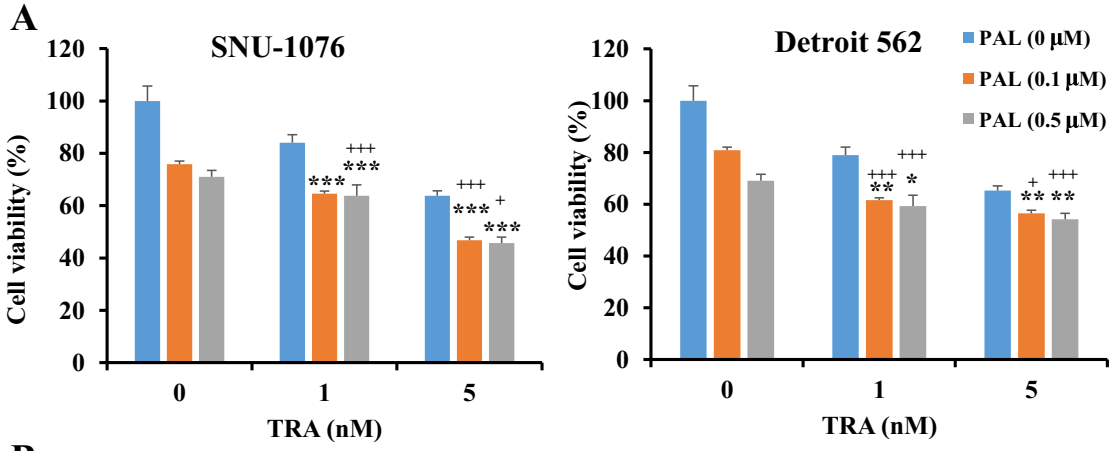

B

CI values of PAL in combination with TRA

PAL (μM)	TRA (nM)	SNU-1076 (CI)	Detroit 562 (CI)
0.1	1	0.23	0.24
	5	0.07	0.14
0.5	1	1.23	0.89
	5	0.35	0.56

C

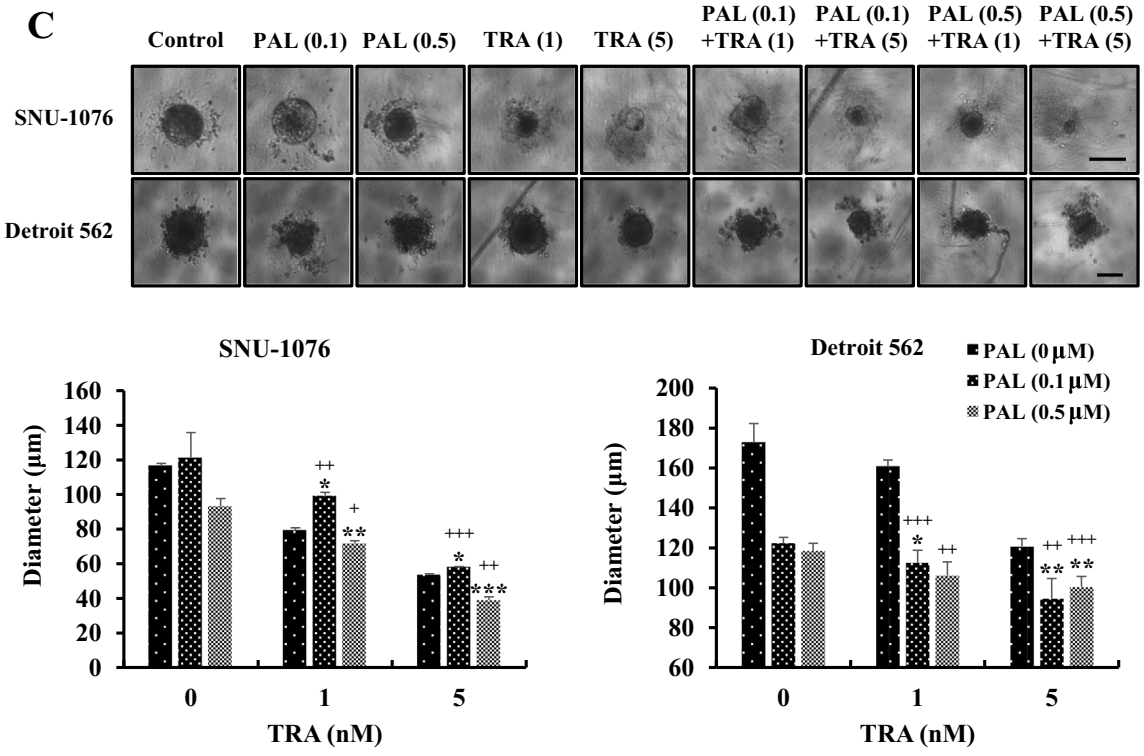

Fig. 1. Synergistic cytotoxic effects of PAL and TRA against HNC cells. (A) HNC cells were treated with PAL (0.1 or 0.5 μM) and/or TRA (1 or 5 nM) for 72 h. MTT assay was performed to determine the cytotoxic effects of PAL and TRA. (B) The combination index (CI) values for PAL and TRA in HNC cells were determined using CompuSyn software (Biosoft). CI value <1 indicated synergistic effects. Data are expressed as the mean ± S.D. of triplicate wells. (C) HNC cells were seeded in ultra-round detachment plates and treated with PAL (0.1 or 0.5 μM) and/or TRA (1 or 5 nM) for 7 days. Cell size (diameter) was measured by optical microscopy. Original magnification of histological images is 40 x; scale bar 100 μm. The combination of PAL and TRA exerted synergistic effects on both 2D and 3D cultures. The data are representatives of three independent experiments. $^{*}P < .05$, $^{**}P < .01$, and $^{***}P < .001$ for PAL vs. Combo group; $^{+}P < .05$, $^{++}P < .01$, and $^{+++}P < .001$ for TRA vs. Combo group.

the cell cycle pathway, we evaluated the expression of cell cycle regulatory molecules such as p-Rb, cyclin B1, and Forkhead box protein M1 (FOXM1). Given that TRA inhibits the MAPK pathway, we measured the level of a well-known MAPK pathway molecule, p-ERK. We found that PAL drastically decreased the expression of cell cycle regulatory molecules, whereas TRA significantly decreased the level of p-ERK. The levels of these

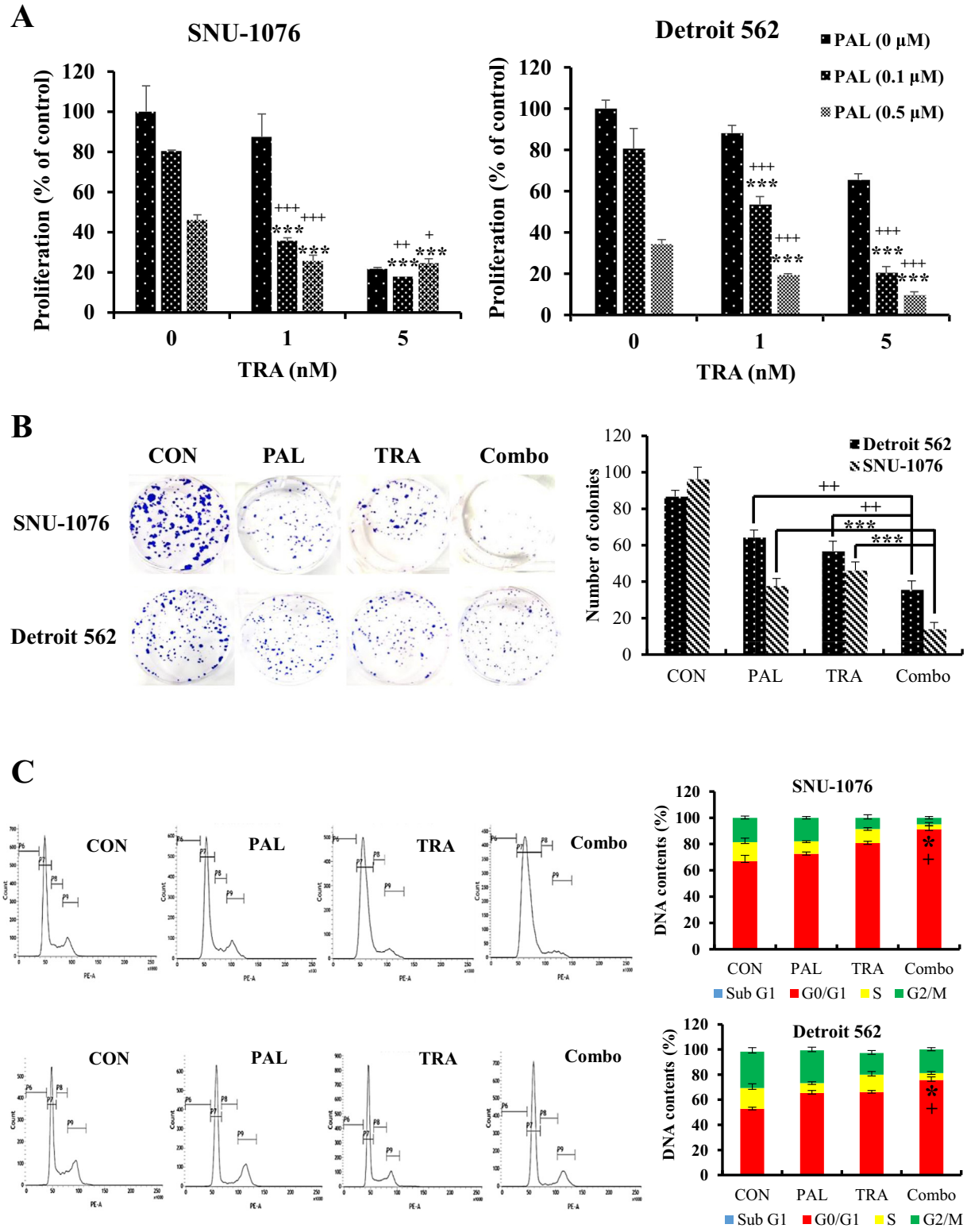

Fig. 2. Synergistic anti-proliferative effects of PAL and TRA on HNC cells. (A) HNC cells were treated with PAL (0.1 or 0.5 μM) and/or TRA (1 or 5 nM) for 96 h. BrdU assay was performed to determine the anti-proliferative effects of PAL and TRA. (B) HNC cells were seeded in 10-cm plates, and treated with PAL (0.1 μM) and/or TRA (5 nM) for 3 days. The cells were then re-seeded into six-well plates and cultured for 14 days. The number of colonies (~50 cells/colony) was counted and analyzed. (C) HNC cells were treated with PAL (0.1 μM)and/or TRA (5 nM) for 72 h. The cell cycle distribution was assessed by flow cytometry, and the DNA content (%) at each phase was analyzed. The data are representative of three independent experiments. *P < .05, **P < .01, and ***P < .001 for PAL vs. Combo group; $^{+}$P < .05, $^{++}$P < .01, and $^{+++}$P < .001 for TRA vs. Combo group.

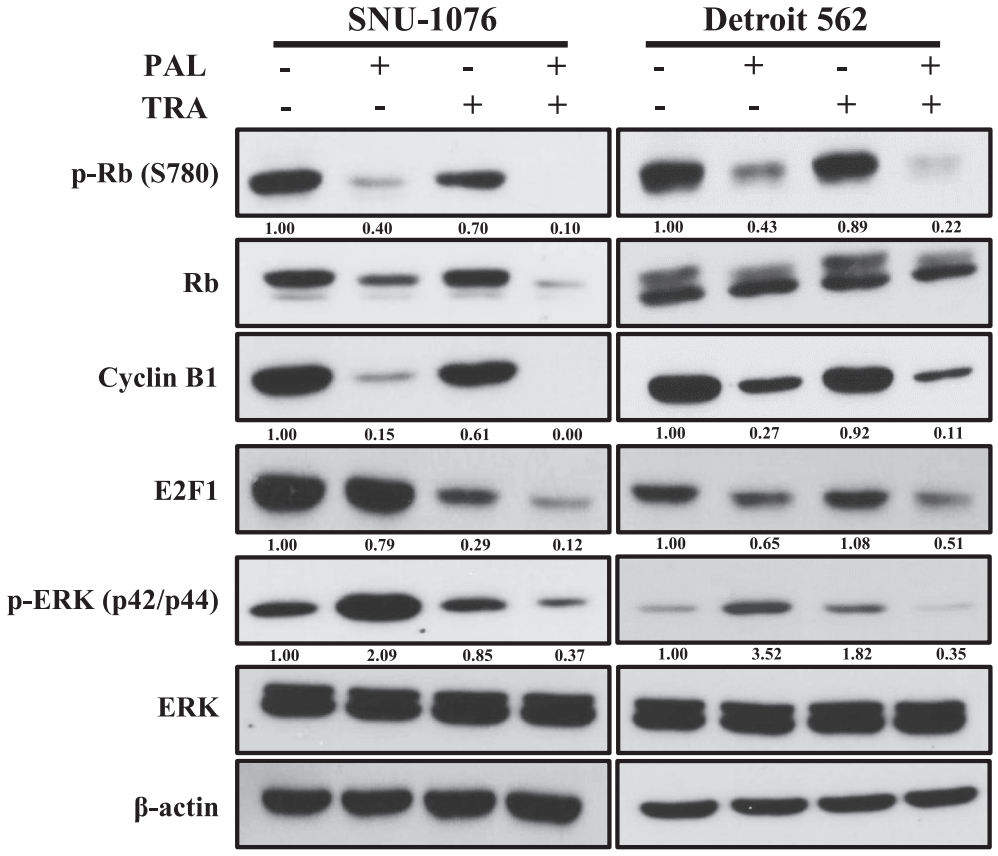

Fig. 3. Inhibition of cell cycle and MAPK signaling pathways by the combination of PAL and TRA in HNC cells. HNC cells were treated with PAL and/or TRA for 72 h. Cell lysates were prepared and the levels of cyclin B1, E2F1, ERK, p-ERK, Rb, and p-Rb were analyzed by western blotting. The data are representatives of two independent experiments.

molecules were completely suppressed following cotreatment with both agents, suggestive of their synergistic activity.

4. Discussion

Alterations in cell cycle-associated genes, including those encoding TP53, p16, and cyclins, are common in HNC. These changes encourage the use of cell cycle inhibitors as potential therapeutic targets for HNC. Inhibitors of specific components of cell cycle have been developed and approved for use in the clinical setting [21]. In particular, PAL, a CDK4/6 inhibitor, has shown anti-proliferative and antitumor effects in various cancers, including HNC. However, PAL failed to exhibit sufficient protection, and development of resistance in cancer cells through reactivation of the MAPK/ERK pathway has been reported [20]. In this direction, we investigated whether the combination of PAL and TRA exerts potent effects on HNC. Our results show that the combination of PAL and TRA could synergistically inhibit HNC cell proliferation by inducing G1 arrest and apoptosis. This combination also enhanced the anticancer effects through inhibition of the CDK/Rb pathway along with the MAPK/ERK signaling pathway. Furthermore, it synergistically inhibited the growth of tumors in an animal model of HNC.

Studies have been performed to investigate the effects of PAL in combination with other agents against cancers [22–24]. PAL has been recommended as a novel candidate drug for the treatment of HNC such as nasopharyngeal carcinoma, as evident from the results of integrated genomic analyses [25]. On the basis of these observations, some studies have attempted to evaluate the efficacy of the combination of PAL and other drugs as treatment regimens. For instance, PAL has been combined with cetuximab (EGFR inhibitor), PF-04691502 (PI3K inhibitor), and carboplatin, but no noticeable benefits have been reported in HNC [15,26,27]. Hence, our strategy of cotreatment with PAL and TRA is meaningful to curb HNC. The results of our study show that the combination of PAL and TRA significantly inhibited the growth of HNC cells as compared with treatment using either agent. We calculated CI values to characterize the synergistic effects of PAL and TRA, and found that the combination of 0.1 μM PAL and 5 nM TRA was the most effective regimen against SNU-1076 and Detroit 562 cells. Based on the optimal concentrations of the two agents, the anti-proliferative effects of PAL and TRA were confirmed by clonogenic survival and BrdU proliferation assays.

CDK4/6 are important cell cycle regulators and perform pivotal roles in the transition from G1 to S phase. These molecules bind to cyclin D and form the CDK4/6-cyclin D complex. PAL has been known to disrupt CDK-associated pathways, including formation of the CDK4/6-cyclin D complex. Therefore, we investigated whether cotreatment with PAL and TRA affects cell proliferation via cell cycle arrest. Our study showed that the combination of these two agents synergistically induced G1 phase arrest, probably through the influence of each agent on cell cycle arrest [28,29]. Given that cell proliferation is tightly regulated by the cell cycle machinery, our results show that this effect of the combination treatment on cell cycle arrest could eventually affect cell proliferation and viability, thereby exerting anticancer effects against HNC cells.

Despite the strong evidence on CDK4/6 activation in cancer cells, CDK4/6 inhibition has not been enough to induce cell death, especially apoptosis [30]. However, in the present study, cotreatment with PAL and TRA significantly induced apoptosis of HNC cells, consistent with the observation of increased nuclear fragmentation in the TUNEL staining. As apoptosis is highly regulated by different pro-apoptotic and anti-apoptotic proteins such as members of the inhibitor-of-apoptosis protein (IAP) family,

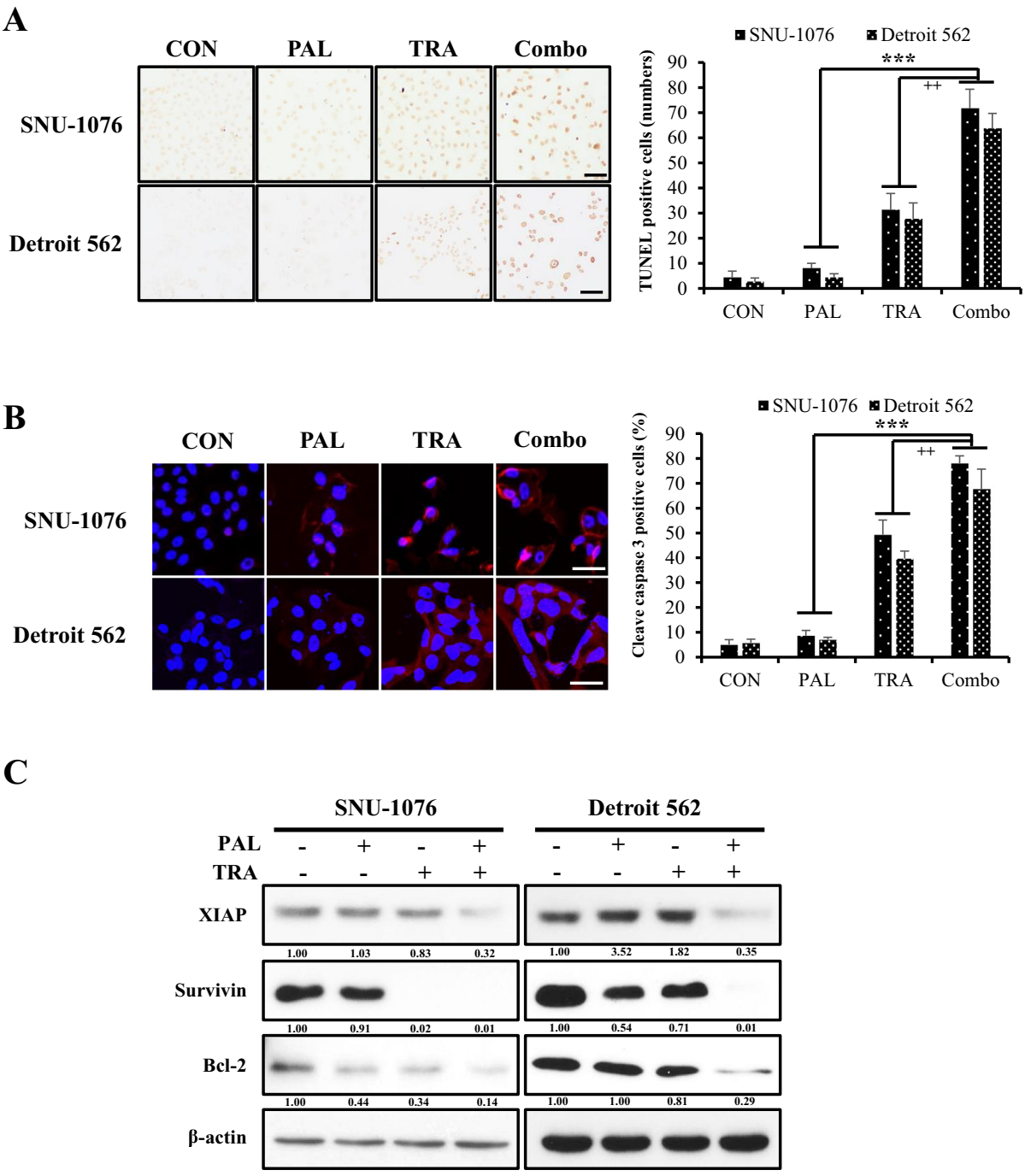

Fig. 4. Induction of apoptosis mediated by the combination of PAL and TRA in HNC cells. (A) HNC cells were treated with PAL (5 μM) and/or TRA (50 nM) for 4 days. TUNEL staining was performed to measure the number of apoptotic cells. Original magnification of histological images is 100 x; scale bar 50 μm. (B) Fluorescence images of cleaved caspase-3 (red) after treatment with PAL and/or TRA in HNC cells. Original magnification of histological images is 200 x; scale bar 50 μm. (C) HNC cells were seeded in 10-cm plates, and then treated with PAL (5 μM) and/or TRA (50 nM) for 4 days. Cell lysates were prepared, and levels of anti-apoptotic molecules such as XIAP, survivin, and Bcl-2 were analyzed by western blotting. (For interpretation of the references to colour in this figure legend, the reader is referred to the web version of this article.)

including XIAP, survivin, and Bcl-2 [31], we investigated whether this combination exerts any effects on these apoptotic molecules. Interestingly, the combination treatment could significantly inhibit the expression of anti-apoptotic molecules such as XIAP, survivin, and Bcl-2 released from the mitochondrion. The synergistic effects of these two agents on apoptosis were in line with the findings of Tao et al. and Lee et al., who found that this combination could enhance apoptosis by changing the expression levels of apoptosis-related molecules in lung and colorectal cancers [23,32]. Although the apoptotic effects of PAL alone are insufficient, increase in the apoptosis level mediated by the combination treatment may be related to the better effects on cell death mediated by TRA after the abnormal regulation of cell cycle by PAL. Taken together, our data show that the combination of PAL and TRA synergistically induced mitochondria-mediated apoptosis in HNC.

Evaluation of the molecular mechanism underlying the effect of this combination regimen revealed a decrease in the levels of Rb, cyclin B1, and E2F1. Thus, these two drugs in combination may downregulate the expression of transcription factors such as E2F1 and FOXM1 that are often

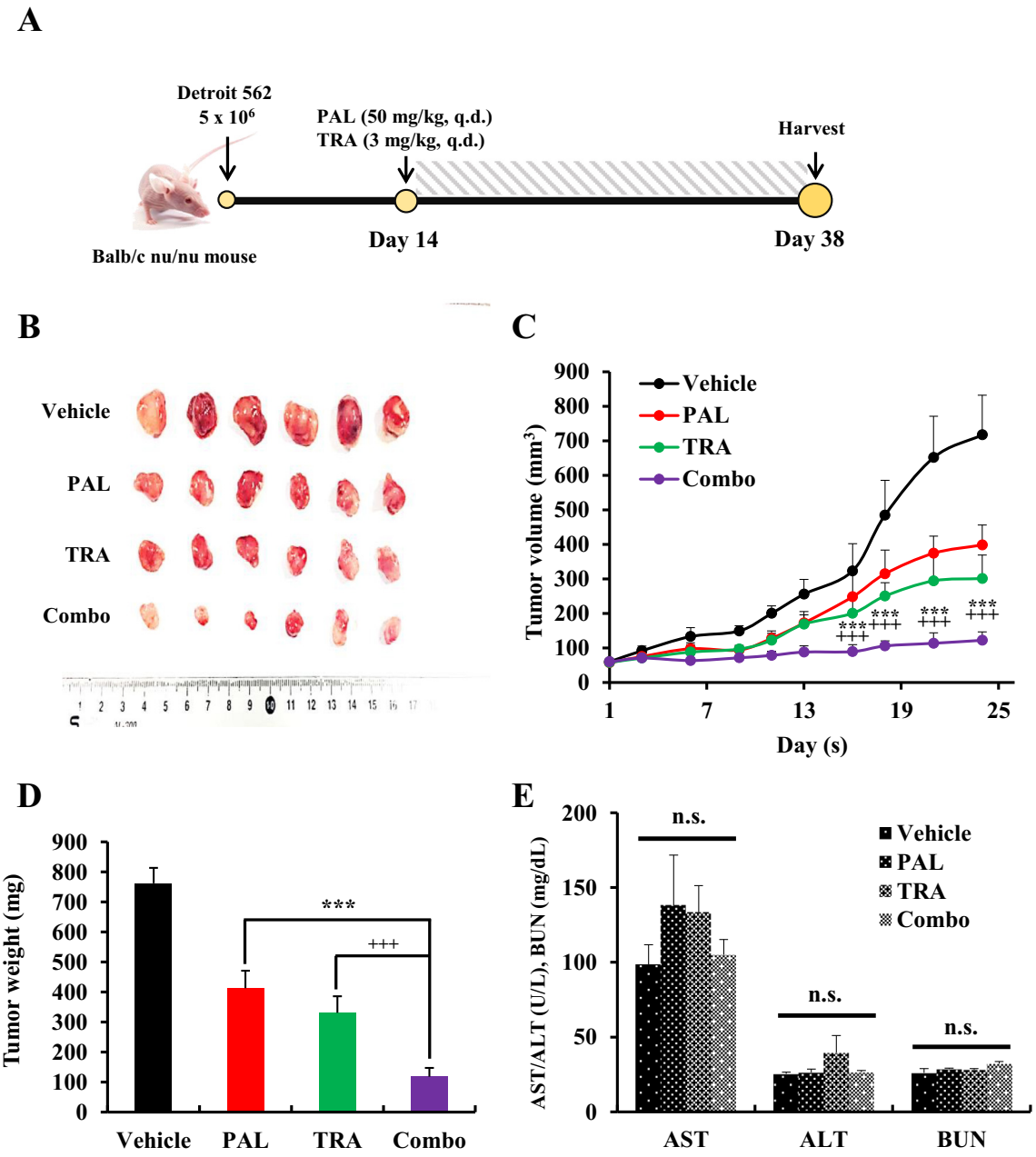

Fig. 5. Inhibition of tumor growth mediated by the combination of PAL and TRA in an HNC xenograft model generated using athymic nude mice. (A) Time schedule and treatment regimen, (B) Representative isolated tumors, (C) tumor growth curve, (D) tumor weight and (E) physiological toxicity in Detroit 562-implanted xenograft mouse. All mice were subjected to a subcutaneous injection of Detroit 562 (5×10^6 cells/200 μL PBS) cells in the flank. As the tumor volume reached between 50 and 100 mm^3, mice were orally administered with PAL (50 mg/kg) and/or TRA (3 mg/kg) for 21 consecutive days. Tumor size was measured every 2 days. Data are represented as the mean ± S.D. ($n = 6$). ***P < .001 for PAL (50 mg/kg) vs. PAL (50 mg/kg) + TRA (3 mg/kg) group and $^{+++}$P < .001 for TRA (3 mg/kg) vs. PAL (50 mg/kg) + TRA (3 mg/kg) group. n.s., non-significant.

overexpressed in HNC [33,34]. Similar results on expression of downstream target molecules have been reported in breast cancer cells cotreated with PAL and the aromatase inhibitor letrozole [35]. CDK4/6 stabilize the transcription factor FOXM1 to maintain the expression of genes involved in the G1/S phase [36], thereby promoting the proliferative mitotic phase and drug resistance through the CDK4/6-Rb-E2F pathway [37–39]. In addition, E2F target genes orchestrate cyclin B1 to control G1 phase through Rb family proteins [40]. Inhibition of the Rb-mediated cytostatic pathway by PAL may contribute to the enhanced anticancer effects of the combination therapy with TRA. We observed that PAL-mediated activation of p-ERK was inhibited after treatment with TRA, thereby enhancing the anticancer effects of PAL on HNC. In the present study, we reveal that the antiproliferative and pro-apoptotic effects of the combination of PAL and TRA were associated with the ability of PAL to enhance the downregulation of the CDK/Rb pathway and that of TRA to inhibit the MAPK/ERK pathway.

In conclusion, to our knowledge, we show for the first time that combined treatment with PAL and TRA significantly inhibited the growth of HNC cells. This drug combination showed synergistic anticancer activities through the inhibition of cell proliferation and induction of apoptosis in vitro *and* in vivo. In addition, combination treatment did not lead to a significant increase in ALT, AST or BUN, thus evident of an acceptable toxicity profile In addition, this combination may augment the therapeutic effect by inhibiting the CDK/Rb and MAPK/ERK signaling pathways. TRA prevented acquired resistance to PAL via blockade of MAPK signaling, suggesting that a combination of these two agents may serve as an important strategy in the clinical setting.

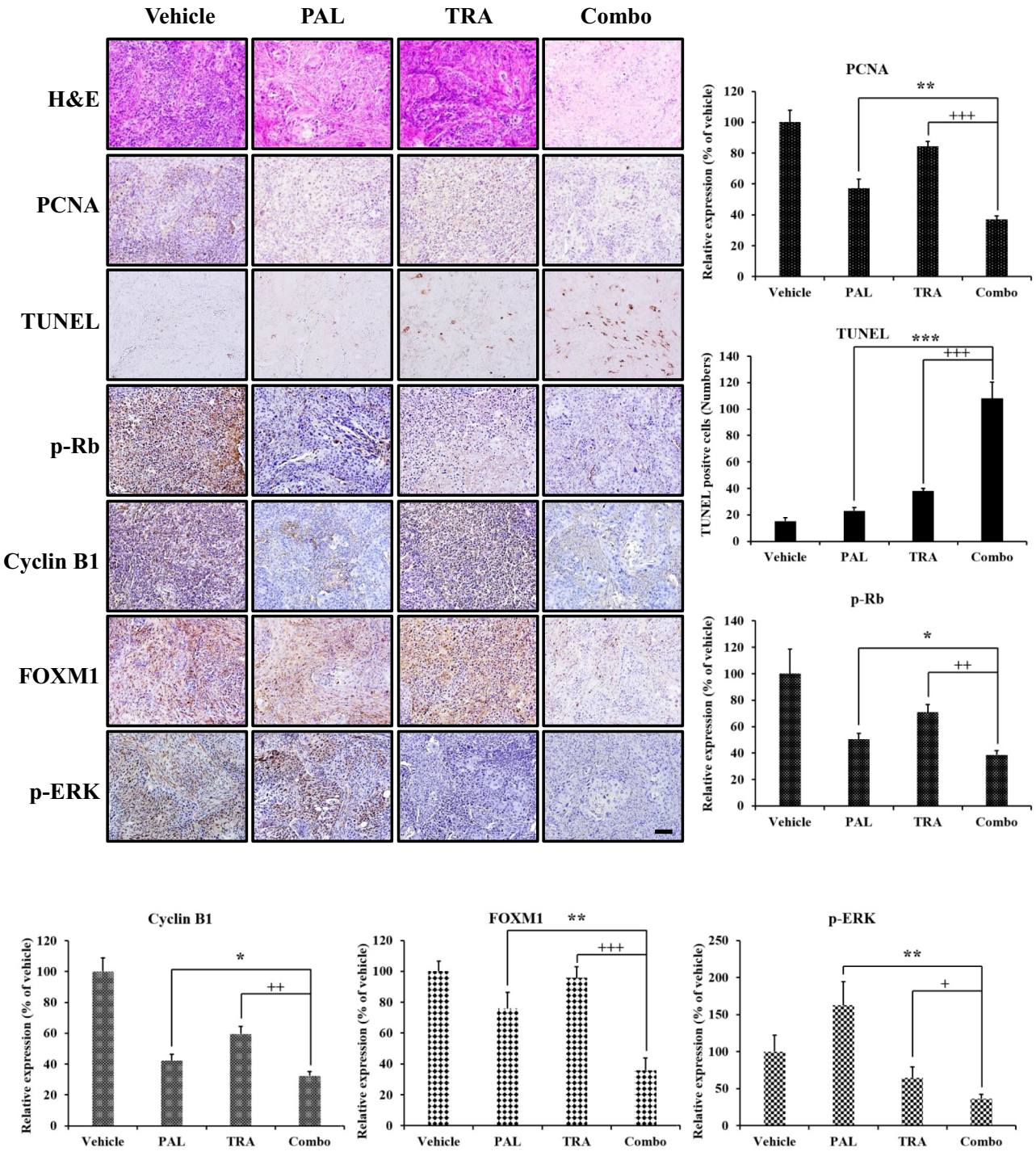

Fig. 6. Antitumor effects of the combination of PAL and TRA in an HNC xenograft model. Histological analysis of xenograft tumor tissues by hematoxylin and eosin (H&E) staining, and immunohistochemical detection of FOXM1, p-Rb, PCNA, TUNEL, cyclin B1, and p-ERK expression. Quantitative analysis was performed with Image J software (n = 6). Relative expression of IHC score Original magnification of histological images is 200 x; scale bar 100 μm.

Acknowledgements

The present study was supported by the National Research Foundation of Korea (2018R1A2A1A05077263, 2019M3E5D1A02069621, 2014009392).

Conflict of Interest

The authors have no conflict of interest to declare.

CRediT author statement.

Zhenghuan Fang: Experimental design, investigation, data curation, and writing draft. Kyung Hee Jung: Experimental design, data curation, and writing-reviewing draft. Ji Eun Lee: Investigation and data curation. Jinhyun Cho: Research plan and strategy. Joo Han Lim: Investigation and validation. Soon-Sun Hong: Writing-Reviewing and editing.

Declaration of competing interests.

The authors that they have NO affiliations with or involvement in any organization or entity with an financial interest (such as honoraria; educational grants; participation in speakers' bureaus; membership, employment, consultancies, stock ownership, or other equity interest; and expert

testimony or patent licensing arrangements), or non-financial interest (such as personal or professional relationships, affiliations, knowledge or beliefs) in the subject matter or materials discussed in this manuscript.

References

[1] A.P. Stein, S. Saha, J.L. Kraninger, A.D. Swick, M. Yu, P.F. Lambert, R.J. Kimple, Prevalence of Human Papillomavirus in Oropharyngeal Cancer: A Systematic Review, Cancer J. 21 (2015) 138–146.

[2] C. Fitzmaurice, C. Allen, R.M. Barber, L. Barregard, Z.A. Bhutta, H. Brenner, D.J. Dicker, O. Chimed-Orchir, R. Dandona, L. Dandona, T. Fleming, M.H. Forouzanfar, J. Hancock, R.J. Hay, R. Hunter-Merrill, C. Huynh, H.D. Hosgood, C.O. Johnson, J.B. Jonas, J. Khubchandani, G.A. Kumar, M. Kutz, Q. Lan, H.J. Larson, X. Liang, S.S. Lim, A.D. Lopez, M.F. MacIntyre, L. Marczak, N. Marquez, A.H. Mokdad, C. Pinho, F. Pourmalek, J.A. Salomon, J.R. Sanabria, L. Sandar, B. Sartorius, S.M. Schwartz, K.A. Shackelford, K. Shibuya, J. Stanaway, C. Steiner, J. Sun, K. Takahashi, S.E. Vollset, T. Vos, J.A. Wagner, H. Wang, R. Westerman, H. Zeeb, L. Zoeckler, F. Abd-Allah, M.B. Ahmed, S. Alabed, N.K. Alam, S.F. Aldhahri, G. Alem, M.A. Alemayohu, R. Ali, R. Al-Raddadi, A. Amare, Y. Amoako, A. Artaman, H. Asayesh, N. Atnafu, A. Awasthi, H.B. Saleem, A. Barac, N. Bedi, I. Bensenor, A. Berhane, E. Bernabe, B. Betsu, A. Binagwaho, D. Boneya, I. Campos-Nonato, C. Castaneda-Orjuela, F. Catala-Lopez, P. Chiang, C. Chibueze, A. Chitheer, J.Y. Choi, B. Cowie, S. Damtew, J. das Neves, S. Dey, S. Dharmaratne, P. Dhillon, E. Ding, T. Driscoll, D. Ekwueme, A.Y. Endries, M. Farvid, F. Farzadfar, J. Fernandes, F. Fischer, G.H. TT, A. Gebru, S. Gopalani, A. Hailu, M. Horino, N. Horita, A. Husseini, I. Huybrechts, M. Inoue, F. Islami, M. Jakovljevic, S. James, M. Javanbakht, S.H. Jee, A. Kasaeian, M.S. Kedir, Y.S. Khader, Y.H. Khang, D. Kim, J. Leigh, S. Linn, R. Lunevicius, H.M.A. El Razek, R. Malekzadeh, D.C. Malta, W. Marcenes, D. Markos, Y.A. Melaku, K.G. Meles, W. Mendoza, D.T. Mengiste, T.J. Meretoja, T.R. Miller, K.A. Mohammad, A. Mohammadi, S. Mohammed, M. Moradi-Lakeh, G. Nagel, D. Nand, Q. Le Nguyen, S. Nolte, F.A. Ogbo, K.E. Oladimeji, E. Oren, M. Pa, E.K. Park, D.M. Pereira, D. Plass, M. Qorbani, A. Radfar, A. Rafay, M. Rahman, S.M. Rana, K. Soreide, M. Satpathy, M. Sawhney, S.G. Sepanlou, M.A. Shaikh, J. She, I. Shiue, H.R. Shore, M.G. Shrime, S. So, S. Soneji, V. Stathopoulou, K. Stroumpoulis, M.B. Sufiyan, B.L. Sykes, R. Tabares-Seisdedos, F. Tadese, B.A. Tedla, G.A. Tessema, J.S. Thakur, B.X. Tran, K.N. Ukwaja, B.S.C. Uzochukwu, V.V. Vlassov, E. Weiderpass, M. Wubshet Terefe, H.G. Yebyo, H.H. Yimam, N. Yonemoto, M.Z. Younis, C. Yu, Z. Zaidi, M.E.S. Zaki, Z.M. Zenebe, C.J.L. Murray, M. Naghavi, Global, Regional, and National Cancer Incidence, Mortality, Years of Life Lost, Years Lived With Disability, and Disability-Adjusted Life-years for 32 Cancer Groups, 1990 to 2015: A Systematic Analysis for the Global Burden of Disease Study, JAMA Oncol. 3 (2017) 524–548.

[3] A.G. Shuman, P. Entezami, A.S. Chernin, N.E. Wallace, J.M. Taylor, N.D. Hogikyan, Demographics and efficacy of head and neck cancer screening, Otolaryngol Head Neck Surg. 143 (2010) 353–360.

[4] Comprehensive genomic characterization of head and neck squamous cell carcinomas, Nature 517 (2015) 576–582.

[5] A.M. Narasimha, M. Kaulich, G.S. Shapiro, Y.J. Choi, P. Sicinski, S.F. Dowdy, Cyclin Dactivates the Rb tumor suppressor by mono-phosphorylation, Elife 3, 2014.

[6] S.J. Weintraub, K.N. Chow, R.X. Luo, S.H. Zhang, S. He, D.C. Dean, Mechanism of active transcriptional repression by the retinoblastoma protein, Nature 375 (1995) 812–815.

[7] S.W. Hiebert, S.P. Chellappan, J.M. Horowitz, J.R. Nevins, The interaction of RB with E2F coincides with an inhibition of the transcriptional activity of E2F, Genes Dev. 6 (1992) 177–185.

[8] R. Barroso-Sousa, G.I. Shapiro, S.M. Tolaney, Clinical Development of the CDK4/6 Inhibitors Ribociclib and Abemaciclib in Breast Cancer, Breast Care (Basel) 11 (2016) 167–173.

[9] C.L. Lee, S. Toomey, A. Farrelly, B. Hennessy, Preclinical drug testing and clinical trial planning of palbociclib (CDK4/6 inhibitor) drug combination with a PI3K or MAPK inhibitor for colorectal cancer (CRC), Ann. Oncol. 30 (2019) i7.

[10] Y. Kong, X. Sheng, X. Wu, J. Yan, M. Ma, J. Yu, L. Si, Z. Chi, C. Cui, J. Dai, Y. Li, H. Yu, T. Xu, H. Tang, B. Tang, L. Mao, B. Lian, X. Wang, X. Yan, S. Li, J. Guo, Frequent Genetic Aberrations in the CDK4 Pathway in Acral Melanoma Indicate the Potential for CDK4/6 Inhibitors in Targeted Therapy, Clin. Cancer Res. 23 (2017) 6946–6957.

[11] A.C. Garrido-Castro, S. Goel, CDK4/6 Inhibition in Breast Cancer: Mechanisms of Response and Treatment Failure, Curr. Breast Cancer Rep. 9 (2017) 26–33.

[12] B.M. Ku, S.Y. Yi, J. Koh, Y.H. Bae, J.M. Sun, S.H. Lee, J.S. Ahn, K. Park, M.J. Ahn, The CDK4/6 inhibitor LY2835219 has potent activity in combination with mTOR inhibitor in head and neck squamous cell carcinoma, Oncotarget 7 (2016) 14803–14813.

[13] X. Gong, L.M. Litchfield, Y. Webster, L.C. Chio, S.S. Wong, T.R. Stewart, M. Dowless, J. Dempsey, Y. Zeng, R. Torres, K. Boehnke, C. Mur, C. Marugan, C. Baquero, C. Yu, S.M. Bray, I.H. Wulur, C. Bi, S. Chu, H.R. Qian, P.W. Iversen, F.F. Merzoug, X.S. Ye, C. Reinhard, A. De Dios, J. Du, C.W. Caldwell, M.J. Lallena, R.P. Beckmann, S.G. Buchanan, Genomic Aberrations that Activate D-type Cyclins Are Associated with Enhanced Sensitivity to the CDK4 and CDK6 Inhibitor Abemaciclib, Cancer Cell 32 (2017) 761–776.

[14] T.N. Beck, R. Georgopoulos, E.I. Shagisultanova, D. Sarcu, E.A. Handorf, C. Dubyk, M.N. Lango, J.A. Ridge, I. Astsaturov, I.G. Serebriiskii, B.A. Burtness, R. Mehra, E.A. Golemis, EGFR and RB1 as Dual Biomarkers in HPV-Negative Head and Neck Cancer, Mol. Cancer Ther. 15 (2016) 2486–2497.

[15] D. Adkins, J. Ley, P. Neupane, F. Worden, A.G. Sacco, K. Palka, J.E. Grilley-Olson, R. Maggiore, N.N. Salama, K. Trinkaus, B.A. Van Tine, C.E. Steuer, N.F. Saba, P. Oppelt, Palbociclib and cetuximab in platinum-resistant and in cetuximab-resistant human papillomavirus-unrelated head and neck cancer: a multicentre, multigroup, phase 2 trial, Lancet Oncol. 20 (2019) 1295–1305.

[16] Y. Sun, W.Z. Liu, T. Liu, X. Feng, N. Yang, H.F. Zhou, Signaling pathway of MAPK/ERK in cell proliferation, differentiation, migration, senescence and apoptosis, J. Recept. Signal Transduct. Res. 35 (2015) 600–604.

[17] T. Chiba, Y. Soeno, Y. Shirako, H. Sudo, H. Yagishita, Y. Taya, S. Kawashiri, Y. Okada, K. Imai, MALT1 Inhibition of Oral Carcinoma Cell Invasion and ERK/MAPK Activation, J. Dent. Res. 95 (2016) 446–452.

[18] J.N. Lavoie, G. L'Allemain, A. Brunet, R. Muller, J. Pouyssegur, Cyclin D1 expression is regulated positively by the p42/p44MAPK and negatively by the p38/HOGMAPK pathway, J. Biol. Chem. 271 (1996) 20608–20616.

[19] J.T. Winston, S.R. Coats, Y.Z. Wang, W.J. Pledger, Regulation of the cell cycle machinery by oncogenic ras, Oncogene 12 (1996) 127–134.

[20] R. de Leeuw, C. McNair, M.J. Schiewer, N.P. Neupane, L.J. Brand, M.A. Augello, Z. Li, L.C. Cheng, A. Yoshida, S.M. Courtney, E.S. Hazard, G. Hardiman, M.H. Hussain, J.A. Diehl, J.M. Drake, W.K. Kelly, K.E. Knudsen, MAPK Reliance via Acquired CDK4/6 Inhibitor Resistance in Cancer, Clin. Cancer Res. 24 (2018) 4201–4214.

[21] J.A. Beaver, L. Amiri-Kordestani, R. Charlab, W. Chen, T. Palmby, A. Tilley, J.F. Zirkelbach, J. Yu, Q. Liu, L. Zhao, J. Crich, X.H. Chen, M. Hughes, E. Bloomquist, S. Tang, R. Sridhara, P.G. Kluetz, G. Kim, A. Ibrahim, R. Pazdur, P. Cortazar, FDA Approval: Palbociclib for the Treatment of Postmenopausal Patients with Estrogen Receptor-Positive, HER2-Negative Metastatic Breast Cancer, Clin. Cancer Res. 21 (2015) 4760–4766.

[22] C.A. Martin, C. Cullinane, L. Kirby, S. Abuhammad, E.J. Lelliott, K. Waldeck, R.J. Young, N. Brajanovski, D.P. Cameron, R. Walker, E. Sanij, G. Poortinga, R.D. Hannan, R.B. Pearson, R.J. Hicks, G.A. McArthur, K.E. Sheppard, Palbociclib synergizes with BRAF and MEK inhibitors in treatment naive melanoma but not after the development of BRAF inhibitor resistance, Int. J. Cancer 142 (2018) 2139–2152.

[23] M.S. Lee, T.L. Helms, N. Feng, J. Gay, Q.E. Chang, F. Tian, J.Y. Wu, C. Toniatti, T.P. Heffernan, G. Powis, L.N. Kwong, S. Kopetz, Efficacy of the combination of MEK and CDK4/6 inhibitors in vitro and in vivo in KRAS mutant colorectal cancer models, Oncotarget 7 (2016) 39595–39608.

[24] Q. Guo, X. Lin, L. Ye, R. Xu, Y. Dai, Y. Zhang, Q. Chen, Comparative Efficacy of CDK4/6 Inhibitors Plus Aromatase Inhibitors Versus Fulvestrant for the First-Line Treatment of Hormone Receptor-Positive Advanced Breast Cancer: A Network Meta-Analysis, Target. Oncol. 14 (2019) 139–148.

[25] C.L. Hsu, K.W. Lui, L.M. Chi, Y.C. Kuo, Y.K. Chao, C.N. Yeh, L.Y. Lee, Y. Huang, T.L. Lin, M.Y. Huang, Y.R. Lai, Y.M. Yeh, H.C. Fan, A.C. Lin, Y.J. Lu, C.H. Hsieh, K.P. Chang, N.M. Tsang, H.M. Wang, A.Y. Chang, Y.S. Chang, H.P. Li, Integrated genomic analyses in PDX model reveal a cyclin-dependent kinase inhibitor Palbociclib as a novel candidate drug for nasopharyngeal carcinoma, J. Exp. Clin. Cancer Res. 37 (2018) 233.

[26] H. Li, Z.R. Zhang, Current status and future direction of lymph node dissection in radical surgery for esophageal cancer, J. Thorac. Dis. 11 (2019) S1678–S1682.

[27] P.L. Swiecicki, G. Durm, E. Bellile, A. Bhangale, J.C. Brenner, F.P. Worden, A multicenter phase II trial evaluating the efficacy of palbociclib in combination with carboplatin for the treatment of unresectable recurrent or metastatic head and neck squamous cell carcinoma, Investig. New Drugs (2020)https://doi.org/10.1007/s10637-020-00898-2.

[28] D. Cretella, C. Fumarola, M. Bonelli, R. Alfieri, S. La Monica, G. Digiacomo, A. Cavazzoni, M. Galetti, D. Generali, P.G. Petronini, Pre-treatment with the CDK4/6 inhibitor palbociclib improves the efficacy of paclitaxel in TNBC cells, Sci. Rep. 9 (2019) 13014.

[29] M. Watanabe, Y. Sowa, M. Yogosawa, T. Sakai, Novel MEK inhibitor trametinib and other retinoblastoma gene (RB)-reactivating agents enhance efficacy of 5-fluorouracil on human colon cancer cells, Cancer Sci. 104 (2013) 687–693.

[30] K. Tamura, Differences of cyclin-dependent kinase 4/6 inhibitor, palbociclib and abemaciclib, in breast cancer, Jpn. J. Clin. Oncol. 49 (2019) 993–998.

[31] C.H.A. Cheung, Y.C. Chang, T.Y. Lin, S.M. Cheng, E. Leung, Anti-apoptotic proteins in the autophagic world: an update on functions of XIAP, Survivin, and BRUCE, J. Biomed. Sci. 27 (2020) 31.

[32] Z. Tao, J.M. Le Blanc, C. Wang, T. Zhan, H. Zhuang, P. Wang, Z. Yuan, B. Lu, Coadministration of Trametinib and Palbociclib Radiosensitizes KRAS-Mutant Non-Small Cell Lung Cancers In Vitro and In Vivo, Clin. Cancer Res. 22 (2016) 122–133.

[33] T.N. Beck, E.A. Golemis, Genomic insights into head and neck cancer, Cancers Head Neck 1 (2016) 1.

[34] C. Pilarsky, M. Wenzig, T. Specht, H.D. Saeger, R. Grutzmann, Identification and validation of commonly overexpressed genes in solid tumors by comparison of microarray data, Neoplasia 6 (2004) 744–750.

[35] R.S. Finn, M. Martin, H.S. Rugo, S. Jones, S.A. Im, K. Gelmon, N. Harbeck, O.N. Lipatov, J.M. Walshe, S. Moulder, E. Gauthier, D.R. Lu, S. Randolph, V. Dieras, D.J. Slamon, Palbociclib and Letrozole in Advanced Breast Cancer, N. Engl. J. Med. 375 (2016) 1925–1936.

[36] L. Anders, N. Ke, P. Hydbring, Y.J. Choi, H.R. Widlund, J.M. Chick, H. Zhai, M. Vidal, S.P. Gygi, P. Braun, P. Sicinski, A systematic screen for CDK4/6 substrates links FOXM1 phosphorylation to senescence suppression in cancer cells, Cancer Cell 20 (2011) 620–634.

[37] M. Tategu, H. Nakagawa, K. Sasaki, R. Yamauchi, S. Sekimachi, Y. Suita, N. Watanabe, K. Yoshid, Transcriptional regulation of human polo-like kinases and early mitotic inhibitor, J. Genet. Genomics 35 (2008) 215–224.

[38] B.D. Cholewa, X. Liu, N. Ahmad, The role of polo-like kinase 1 in carcinogenesis: cause or consequence? Cancer Res. 73 (2013) 6848–6855.

[39] C. Michaloglou, C. Crafter, R. Siersbaek, O. Delpuech, J.O. Curwen, L.S. Carnevalli, A.D. Staniszewska, U.M. Polanska, A. Cheraghchi-Bashi, M. Lawson, I. Chernukhin, R. McEwen, J.S. Carroll, S.C. Cosulich, Combined Inhibition of mTOR and CDK4/6 Is Required for Optimal Blockade of E2F Function and Long-term Growth Inhibition in Estrogen Receptor-positive Breast Cancer, Mol. Cancer Ther. 17 (2018) 908–920.

[40] C. Lukas, C.S. Sorensen, E. Kramer, E. Santoni-Rugiu, C. Lindeneg, J.M. Peters, J. Bartek, J. Lukas, Accumulation of cyclin B1 requires E2F and cyclin-A-dependent rearrangement of the anaphase-promoting complex, Nature 401 (1999) 815–818.